Edge effects on sandwich composites

Moussa Karama, Sébastien Mistou

Laboratoire Genie de Production, Ecole Nationale d'Ingénieurs de Tarbes, BP 1629, 65016 Tarbes Cedex, France. moussa@enit.fr

Abstract
One of the current problems connected with sandwich multilayered composite materials concerns the analysis of the stress distribution around singularities such as free or loaded edge. The research carried out was focused on a comparative study between a numerical and an experimental approach. The results obtained with photoelasticimetry are in good agreement with analytical and numerical models and highlight some problems to consider in this characterisation methodology.
Keywords : Composites, Sandwich, Edge Effects, Photoelasticimetry.

Introduction

Composite materials are employed more and more in the design of light structures which need a high mechanical strength. Research on composites have resulted in diverse analytical models, the main problem of which, is how to take into account the transverse shear effects. However, when designing the sandwich composite structures, it is necessary to verify the load transfer process in order to calculate the dimensions of the structure and to account for edge effects.
Work on these problems resulted in the development of several models which do or do not satisfy the continuity of the stresses at layer interfaces whose mechanical properties are different. These models are compared with exact theories of Pagano (1969), Srinivas (1970) and, Ren (1987), or with numerical simulations, but rarely with experimental references.
With the aim to establish experimental references on sandwich composites in statics and then in dynamics, tests in bending are developped. At the beginning, the principal purposes are to apply different characterisation methodology, such as photoelasticimetry, on sandwich composite beams and to compare results obtained by the three methods (analytical model, numerical calculations on Ansys and experimental tests), and to emphasize edge effects.

Analytical Model

Di Sciuva (1987,1993) and then Touratier (1991,1992) proposed simplified discrete layer models with only five variational unknowns (two membrane displacements, a transverse displacement and two rotations). Nevertheless, in these two cases, the compatibility conditions both at layer interfaces and on the frontiers cannot be satisfied. He (1994) introduced the Heaviside step function which allows automatic verification of the displacement continuity at interfaces between different layers.
The new discrete layer model presented comes from the work of Ossadzow (1996), Karama (1997,1998) and Mistou (1999), the displacement field is :

$$\begin{aligned} U_1(x_1,x_3,t) &= u_1^0(x_1,t) - x_3 w_{,1}(x_1,t) + h_1(x_3)\varphi_1(x_1,t) \\ U_2 &= 0 \\ U_3(x_1,t) &= w(x_1,t) \end{aligned} \tag{1}$$

with transverse shear function :

$$h_1(x_3) = g(x_3) + \sum_{m=1}^{N-1} \lambda_1^{(m)} \left[-\frac{x_3}{2} + \frac{f(x_3)}{2} + (x_3 - x_{3_{(m)}}) H(x_3 - x_{3_{(m)}}) \right] \tag{2}$$

and, $f(x_3) = \frac{h}{\pi} \sin \frac{\pi x_3}{h}$ shear refinement sine function, $g(x_3) = \frac{h}{\pi} \cos \frac{\pi x_3}{h}$ membrane refinement cosine function, $H(x_3 - x_{3_{(m)}})$ Heaviside step function.

The coefficients $\lambda_1^{(m)}$ are determined with the boundary conditions on top and bottom faces, and with the continuity conditions at layer interfaces :

$$\sigma_{13}(x_3 = 0) = \sigma_{13}(x_3 = h) = 0 \qquad \sigma_{13}^{(m)}(x_3 = x_{3_{(m)}}) = \sigma_{13}^{(m+1)}(x_3 = x_{3_{(m)}}) \tag{3}$$

From the virtual power principle, the motion equations and the natural boundary conditions can be obtained. The calculations are made in small perturbations.

The principle is : $$\int_\Omega \rho U^{*T} \ddot{U} d\Omega = -\int_\Omega \overline{\overline{D}}^{*T} : \overline{\overline{\sigma}} d\Omega + \int_\Omega U^{*T} f d\Omega + \int_\Gamma U^{*T} \hat{F} d\Gamma \tag{4}$$

From the divergence theorem and the kinematic (1), the different components of the principle (4) can be obtained. The virtual power of acceleration quantities is :

$$P_{(a)}^* = \int_0^L \begin{bmatrix} (I_w \ddot{u}_1^0 + I_{uw'} \ddot{w}_{,1} + I_{u\omega} \ddot{\varphi}_1) u_1^{0*} \\ + (-I_{uw'} \ddot{u}_{1,1}^0 + I_w \ddot{w} - I_{w'} \ddot{w}_{,11} - I_{\omega w'} \ddot{\varphi}_{1,1}) w^* \\ + (I_{u\omega} \ddot{u}_1^0 + I_{\omega w'} \ddot{w}_{,1} + I_\omega \ddot{\varphi}_1) \varphi_1^* \end{bmatrix} dx_1 + (I_{uw'} \ddot{u}_1^0 + I_{w'} \ddot{w}_{,1} + I_{\omega w'} \ddot{\varphi}_1) w^* \tag{5}$$

with, $$\left\{I_w, I_{w'}, I_\omega, I_{uw'}, I_{u\omega}, I_{\omega w'}\right\} = \int_0^h \left\{\rho, \rho x_3^2, \rho h_1^2(x_3), -\rho x_3, \rho h_1(x_3), -\rho x_3 h_1(x_3)\right\} dx_3 \tag{6}$$

The virtual power of internal work is :

$$P_{(i)}^* = \int_0^L (N_{11,1} u_1^{0*} + M_{11,11} w^* + (P_{11,1} - P_{13}) \varphi_1^*) dx_1 - N_{11} u_1^{0*} - M_{11,1} w^* - P_{11} \varphi_1^* + M_{11} w_{,1}^* \tag{7}$$

with, $$\left\{N_{11}, P_{11}, M_{11}, P_{13}\right\} = \int_0^h \left\{\sigma_{11}, h_1(x_3)\sigma_{11}, x_3\sigma_{11}, h_{1,3}(x_3)\sigma_{13}\right\} dx_3 \tag{8}$$

The virtual power of external loading is :

$$P_{(e)}^* = \int_0^L (\overline{n}_1 u_1^{0*} + (\overline{n}_3 + \overline{m}_{1,1}) w^* + \overline{p}_1 \varphi_1^*) dx_1 + \overline{N}_1 u_1^{0*} + (\overline{N}_3 - \overline{m}_1) w^* + \overline{P}_1 \varphi_1^* - \overline{M}_1 w_{,1}^* \tag{9}$$

with, $$\left\{\overline{n}_1, \overline{m}_1, \overline{n}_3, \overline{p}_1, \overline{N}_1, \overline{M}_1, \overline{N}_3, \overline{P}_1\right\} = \int_0^h \left\{f_1, x_3 f_1, f_3, h_1 f_1, F_1, x_3 F_1, F_3, h_1 F_1\right\} dx_3 \tag{10}$$

The three-dimensional orthotropic constitutive law is :

$$\begin{Bmatrix} \sigma_{11} \\ \sigma_{22} \\ \sigma_{33} \\ \sigma_{23} \\ \sigma_{13} \\ \sigma_{12} \end{Bmatrix} = \begin{bmatrix} C_{11} & C_{12} & C_{13} & 0 & 0 & 0 \\ C_{12} & C_{22} & C_{23} & 0 & 0 & 0 \\ C_{13} & C_{23} & C_{33} & 0 & 0 & 0 \\ 0 & 0 & 0 & C_{44} & 0 & 0 \\ 0 & 0 & 0 & 0 & C_{55} & 0 \\ 0 & 0 & 0 & 0 & 0 & C_{66} \end{bmatrix} \begin{Bmatrix} \varepsilon_{11} \\ \varepsilon_{22} \\ \varepsilon_{33} \\ 2\varepsilon_{23} \\ 2\varepsilon_{13} \\ 2\varepsilon_{12} \end{Bmatrix} \tag{11}$$

The dimension x_2 is supposed unitary, and the effects of σ_{33} are neglected, the orthotropic constitutive law (11) is modified as follows :

$$\begin{Bmatrix} \sigma_{11} \\ \sigma_{13} \end{Bmatrix} = \begin{bmatrix} C_{11}' = \dfrac{C_{11}C_{33} - C_{13}^2}{C_{33}} & 0 \\ 0 & C_{55} \end{bmatrix} \begin{Bmatrix} \varepsilon_{11} \\ 2\varepsilon_{13} \end{Bmatrix} \tag{12}$$

From the constitutive law (12) and from equation (8), new values of N_{11}, M_{11}, P_{11} et P_{13} are deduced. These terms constitute the generalized constitutive law :

$$\begin{bmatrix} N_{11} \\ M_{11} \\ P_{11} \\ P_{13} \end{bmatrix} = \begin{bmatrix} A_{11} & B_{11} & \tilde{K} & 0 \\ B_{11} & D_{11} & \tilde{T} & 0 \\ \tilde{K} & \tilde{T} & \tilde{S} & 0 \\ 0 & 0 & 0 & \tilde{Y} \end{bmatrix} \begin{bmatrix} u_{1,1}^0 \\ -w_{,11} \\ \varphi_{1,1} \\ \varphi_1 \end{bmatrix} \tag{13}$$

with, $\left\{A_{11},B_{11},D_{11},\tilde{K},\tilde{T},\tilde{S},\tilde{Y}\right\}=\int_0^h\left\{C'_{11},C'_{11}x_3,C'_{11}x_3^2,C'_{11}h_1,C'_{11}h_1x_3,C'_{11}h_1^2,C_{55}h_{1,3}^2\right\}dx_3$ (14)

Gathering the different components of the principle (5)-(10) and (13), the motion equations obtained are, $\forall u_1^{0*},\forall w^*,\forall\varphi_1^*$, :

$$\begin{aligned}
&I_w\ddot{u}_1^0+I_{uw'}\ddot{w}_{,1}+I_{u\omega}\ddot{\varphi}_1=A_{11}u_{1,11}^0-B_{11}w_{,111}+\tilde{K}\varphi_{1,11}+\bar{n}_1\\
&-I_{uw'}\ddot{u}_{1,1}^0+I_w\ddot{w}-I_{w'}\ddot{w}_{,11}-I_{\omega w'}\ddot{\varphi}_{1,1}=B_{11}u_{1,111}^0-D_{11}w_{,1111}+\tilde{T}\varphi_{1,111}+\bar{n}_3+\bar{m}_{1,1}\\
&I_{u\omega}\ddot{u}_1^0+I_{\omega w'}\ddot{w}_{,1}+I_\omega\ddot{\varphi}_1=\tilde{K}u_{1,11}^0-\tilde{T}w_{,111}+\tilde{S}\varphi_{1,11}-\tilde{Y}\varphi_1+\bar{p}_1
\end{aligned}\tag{15}$$

And the natural boundary conditions are, $\forall u_1^{0*},\forall w^*,\forall\varphi_1^*,\forall w_{,1}^*$, :

$$\begin{aligned}
&0=-A_{11}u_{1,1}^0+B_{11}w_{,11}-\tilde{K}\varphi_{1,1}+\bar{N}_1\\
&I_{uw'}\ddot{u}_1^0+I_{w'}\ddot{w}_{,1}+I_{\omega w'}\ddot{\varphi}_1=-B_{11}u_{1,11}^0+D_{11}w_{,111}-\tilde{T}\varphi_{1,11}+\bar{N}_3-\bar{m}_1\\
&0=-\tilde{K}u_{1,1}^0+\tilde{T}w_{,11}-\tilde{S}\varphi_{1,1}+\bar{P}_1\\
&0=B_{11}u_{1,1}^0-D_{11}w_{,11}+\tilde{T}\varphi_{1,1}-\bar{M}_1
\end{aligned}\tag{16}$$

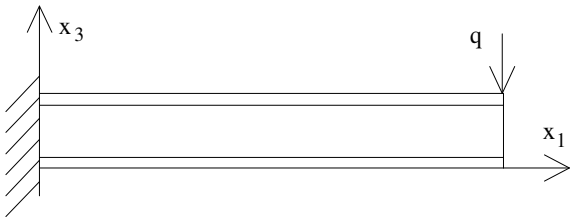

Figure 1 : Clamped free beam under concentrated load

In this case (Fig.1), the value of $\bar{N}_3$ is : $\bar{N}_3=\int_0^h F_3dx_3=q$ (17)

The equation system to solve is deduced from (15) :

$$\begin{aligned}
&0=A_{11}u_{1,11}^0-B_{11}w_{,111}+\tilde{K}\varphi_{1,11}\\
&0=B_{11}u_{1,111}^0-D_{11}w_{,1111}+\tilde{T}\varphi_{1,111}\\
&0=\tilde{K}u_{1,11}^0-\tilde{T}w_{,111}+\tilde{S}\varphi_{1,11}-\tilde{Y}\varphi_1
\end{aligned}\tag{18}$$

Integrating the differential system (18) allows the solutions of u_1^0, w and φ_1 to be obtained. Eight constants are to be also determined by the four natural boundary conditions at the free edge deduced from (16) and (17) :

$$\begin{aligned}
&0=A_{11}u_{1,1}^0-B_{11}w_{,11}+\tilde{K}\varphi_{1,1}\\
&0=B_{11}u_{1,11}^0-D_{11}w_{,111}+\tilde{T}\varphi_{1,11}-q\\
&0=\tilde{K}u_{1,1}^0-\tilde{T}w_{,11}+\tilde{S}\varphi_{1,1}\\
&0=B_{11}u_{1,1}^0-D_{11}w_{,11}+\tilde{T}\varphi_{1,1}
\end{aligned}\tag{19}$$

and by the following kinematic boundary conditions at the clamped edge : w(0)=0, $u_1^0(0)=0$, $w_{,1}(0)=0$, $\varphi_1(0)=0$.

Experimental device

Several optic methods are used for measuring strain field. In the setting of this study, a technique of photoelasticimetry by reflection was used. The principle of photoelasticimetres using reflection does

not differ with that of transmissions. For this study, a digital reading polariscope was acquired. This equipment is provided with a zero compensator by a measurable variable birefringency body interposed on the light route providing the cancellation of the previous effect. It is like the principle of the weighbridge (Fig. 2).

Photoelasticimetry uses the accidental birefringency of a transparent body that becomes birefringent when it is submitted to stresses. Measures on edges are valid provided that they correspond to the edge of the piece and not only of the coating.

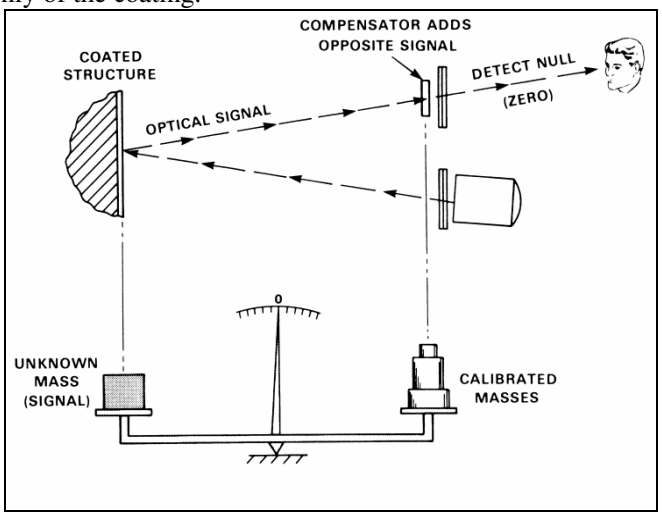

Figure 2 : Principle of the photoelasticimetry by reflection

In photoelasticimetry by coating, the superficial strains on the coating are imposed on the structure. Axes of birefringency of a photoelastic body submitted to strains are also the main directions of strains. The obtaining of results is limited to two types of measures, the main direction measure (with the help of isoclines) and the measure of differences between the main strain (with the help of isochromes).

In the case of non isotropic materials, it is to be noted that the main stresses do not correspond to the main directions of strain measured by isoclines. The order of fringes (isochromes) observed with photoelastic coatings is proportional to the main strain difference and therefore to the surface of the structure (April, 1984). Therefore one has :

$$(\varepsilon_1 - \varepsilon_2) = \text{n.f} \tag{20}$$

where f represents the value of a fringe and is obtained by calibration of photoelastic material, n is the order of fringe given by the spectrum of Newton.
In pure bending, two phenomena occur modifying the photoelastic effect. On the one hand the neutral surface is slightly moved toward the coating, on the other hand, strains are more important to the outside surface than to the surface of bonding (Fig. 3).

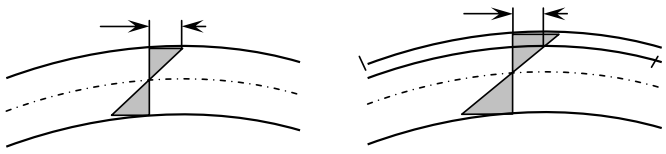

Real strain Measured strain

Figure 3 : Effect of the coating

Two sandwich materials have been studied : the core is an aluminium honeycomb (diameter of 6-mm cells, density 69 kg/m3); skins are in aluminium, adhered by a polyurethane glue. The dimensional features of samples are a total thickness of 21 and 15.8 mm and a skin thickness of 1.5 and 0.8 mm respectively for materials thereafter named Sandwich 1 and Sandwich 2.

Results

At the time of a bending test on Sandwich 1, a photostress plate, of sensitivity f = 665 m/ms, has been bonded on a part of the sample in order to measure strains in the thickness. Figures 4-a and a-b present results obtained respectively for a P load of 300 N, on the thickness of the sample to 20 mm of the clamp, and on the entire length of the sample to 3 mm of the superior skin, either to 1.5 mm of the interface core/skin.

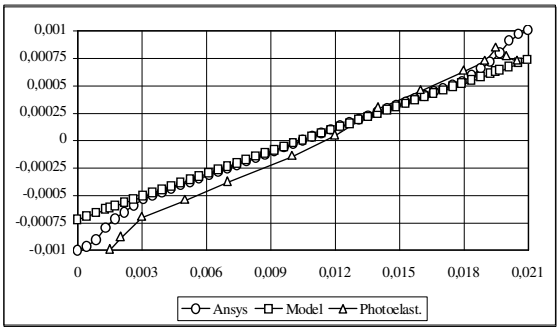

Figure 4-a : Strains in the thickness

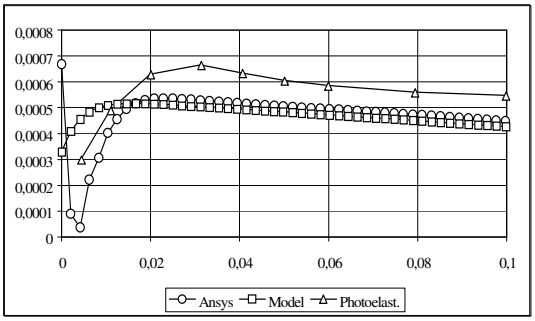

Figure 4-b : Strains according to the length

For the following experience, the type of solicitation is the same as previously, but the sample (Sandwich 2) has a hole 50 mm from the clamped edge and a coating photostress has been bonded on its upper skin. The objective of this test is to observe theeffects of edge while putting in evidence the distribution of strains around the hole and to compare results with the numeric simulation. Figures 6-a and 6-b respectively present distributions according to the transverse and longitudinal axis of the hole.

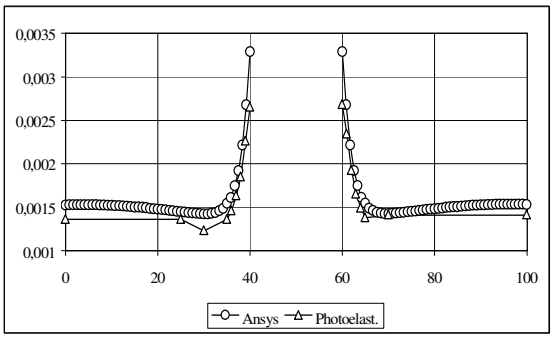

Figure 6-a : Transverse strains

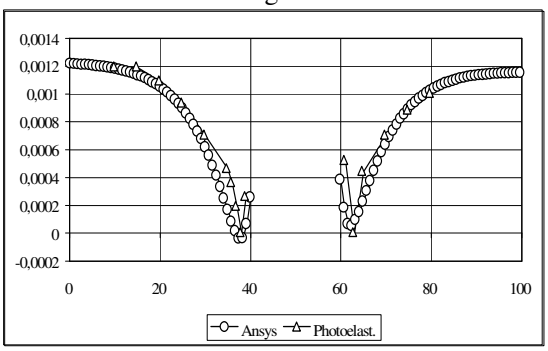

Figure 6-b : Longitudinal strains

Conclusions

Work achieved until then have led to very interesting results for the use of the photoelasticimetry for the experimental validation of numeric and analytic modelization.

The development of the analytic model is simplified by the sine type transverse shear function which permits simple mathematical manipulations while staying accurate because of the x_3 odd power terms which appear in its development. This model is also simple in so far as no correction factor is used as opposed to the higher order models. The innovation in relation to the models proposed in the

bibliography is also the introduction of the membrane refinement cosine function $g(x_3)$ which in fact represents the counterpart of the transverse shear sine function $f(x_3)$. Actually, the function $g(x_3)$ is the same as $f(x_3)$, but with a cosine instead of a sine, which allows the x_3 even power terms to be taken into account. This membrane refinement improves the warping of the straight section in bending deformations. The comparison of the results obtained by the present model, and relative to the Ansys finite element reference model, has demonstrated the accuracy of our model.
The static study in the thickness permitted to visualize bending and not the main strain difference, because of a too large rigidity of the photostress in relation to the honeycomb. A pertinent choice between sandwich and coating is necessary to observe the main strain difference on the thickness of sandwiches and to determine it, thanks to directions, the strain and shear stress.

The second set of tests had for goal the visualization of edge effects in the vicinity of a hole. The photoelasticimetry shows, on the one hand, zones without shear stresses thanks to the exploitation of isoclines, and on the other hand the quality of measures of the main strain difference. The association of the two data, for the calculation of the shear strain and stress, shows a good consistency of results obtained from the exploitation of isoclines and isochromes. The photoelasticimetry seems well adapted to the visualization of edge effects.

References

Avril J., Brulé J.C., Corby T., Dejou G., Dorsey J., Dunand Y., Fleury J., Gérent M., Le Goër J.L., Marcillac G., Perry C., Redner A., Starr J., Whitehead R., Zandman F., Encyclopédie d'analyse des contraintes, Vishay-Micromesures, Edition 1984.
Pagano N.J., Exact solution for composite laminates in cylindrical bending, J. Composite Structures, Vol 14, 1969, pp 61-86.
Ren J.G. , Exact solution for laminated cylindrical shells in cylindrical bending, Composites Science and Technology, 29, 1987, pp 169-187.
Srinivas S., Rao A.K., Bending, vibration and buckling of simply supported thich orthotropic rectangular plates and laminates, Int. J. Solid structures, Vol 6, 1970, pp 1463-1481.
Di Sciuva M., An improved shear-deformation theory for moderately thick multilayered anisotropic shells and plates, ASME Journal Applied Mechanics, vol 54, 1987, pp. 589-596.
Di Sciuva M., A general quadrilateral multilayered plate element with continuous interlaminar stresses, Computers and Structures, vol 47(1), 1993, pp. 91-105.
Touratier M., An efficient standard plate theory, International Journal Engineering Science, vol 29(8), 1991, pp. 901-916.
Touratier M., A generalization of shear deformation theories for axisymmetric multilayered shells, International Journal Solids Structures, vol 29(11), 1992, pp. 1379-1399.
Touratier M., A refined theory of laminated shallow shells, International Journal Solids Structures, vol 29(11), 1992, pp. 1401-1415.
He L.H., A linear theory of laminated shells accounting for continuity of displacements and transverse shear stresses at layer interfaces, International Journal Solids structures, vol 31(5), 1994, pp. 613-627.
Ossadzow C., Modelisation de coques composites multicouches, Ph D Thesis, 1996, Ecole Normale Superieure de Cachan, France.
Karama M., Abou Harb B., Mistou S., Caperaa S., Bending, buckling and free vibration of sandwich composite beams with a transverse shear stress continuity model, Proceedings of Euromech 360 Mechanics of sandwich structures, Saint Etienne, France, May 13-15, 1997, Kluwer Academic Publisher, pp. 97-104.
Karama M., Abou Harb B., Mistou S., Caperaa S., Bending, buckling and free vibration of laminated composite with a transverse shear stress continuity model, Composites Part B Engineering, vol 29(3), 1998, pp. 223-234.
Mistou S., Karama M., Lorrain B., Faye J.P., Analysis of sandwich composite beams with a new transverse shear stress continuity model, Journal of Sandwich Structures and Materials, vol 2, 1999.